



ISSN: 2617-6548

URL: www.ijirss.com



Types of failures of non-critical components and reliability forecasting of locomotives

Olga Kisselyova¹, Seidulla Abdullayev¹, Gabit Bakyt^{2*}, Yermek Baubekov², Zhanar Altayeva¹

¹Satbayev University, Almaty, Republic of Kazakhstan.

²Mukhametzhn Tynyshpayev ALT University, Almaty, Republic of Kazakhstan.

Corresponding author: Gabit Bakyt (Email: gaba_b@bk.ru)

Abstract

The purpose of this article is to consider the main types of failures of load-bearing parts of traction rolling stock, which have a significant impact on the operational reliability and safety of railway transport. In the bearing components of the mechanical part of locomotives, both gradual and sudden failures may occur. The analysis of the causes of failures, fatigue failures, wear, corrosion damage, and manufacturing defects has been performed. Gradual failures arise due to the accumulation of fatigue damage. The methods of increasing the life of the bearing elements and improving the design are proposed. Sudden failures are defined as those associated with a reduction in the safety margin of long-term (static) or impact strength below the permissible value. According to these studies, the probability of a sudden failure is determined as the probability that the random value of the applied static stress exceeds the random value of some characteristic of the material's strength, σ_R , which refers to the yield strength or tensile strength, σ_b . The results of this study can be used in the development of technical measures for the maintenance and repair of locomotives.

Keywords: Fatigue damage, High-speed trains, Material strength, Railway infrastructure, Railway rolling stock, Reliability, and safety.

DOI: 10.53894/ijirss.v8i3.7222

Funding: This research has been/was/is funded by the Science Committee of the Ministry of Science and Higher Education of the Republic of Kazakhstan (Grant No. AP22688234).

History: Received: 31 March 2025 / Revised: 6 May 2025 / Accepted: 8 May 2025 / Published: 20 May 2025

Copyright: © 2025 by the authors. This article is an open access article distributed under the terms and conditions of the Creative Commons Attribution (CC BY) license (<https://creativecommons.org/licenses/by/4.0/>).

Competing Interests: The authors declare that they have no competing interests.

Authors' Contributions: All authors contributed equally to the conception and design of the study. All authors have read and agreed to the published version of the manuscript.

Transparency: The authors confirm that the manuscript is an honest, accurate, and transparent account of the study; that no vital features of the study have been omitted; and that any discrepancies from the study as planned have been explained. This study followed all ethical practices during writing.

Publisher: Innovative Research Publishing

1. Introduction

Ensuring high reliability and safety of the operation of locomotives is one of the priority tasks of railway transport. The key role in this process is played by the load-bearing structural elements such as the frame, bogies, beams, and connecting assemblies, which account for the main mechanical load during the movement of the rolling stock. Failures of these parts can lead not only to significant economic losses but also to the creation of a threat of emergency situations.

In conditions of intensive operation, high dynamic load, and exposure to an aggressive external environment, the technical condition of the load-bearing structural elements, frames, beams, welded joints, and suspensions is of particular

importance. Failure of even one of these components can lead to accidents, serious economic losses, and a threat to traffic safety.

Modern forecasting methods based on the analysis of operational data and the use of digital technologies open up new opportunities for improving the reliability of railway equipment. Predictive diagnostics, machine learning, and real-time status monitoring allow not only the timely identification of potential malfunctions but also the optimization of repair schedules, reducing costs and increasing the availability rate of locomotives.

The research aims to identify the most common types of failures of load-bearing parts of locomotives, determine the factors influencing their occurrence, and develop and test reliability forecasting methods using modern analytical and digital tools. The results of the work can be used to optimize maintenance regulations and improve the efficiency of rolling stock operation.

The reliability of the operated fleet of traction rolling stock is one of the key factors in ensuring the stable and safe operation of railway transport. In conditions of increasing traffic intensity and increasing complexity of traction rolling stock structures, the requirements for the strength and durability of the supporting parts of locomotives are increasing. Emergencies resulting from failures of such elements can lead to serious economic losses, disruption of traffic schedules and a threat to the lives of maintenance personnel [1, 2].

The need for the development of high-speed and very high-speed train services, along with the construction of new railway lines, requires significant additional investments. One of the key factors for the innovative development of the railway industry is the emphasis on reliability, operational readiness, maintainability, and safety, particularly with respect to its infrastructure. Additionally, in accordance with the transportation system development strategy of the Republic of Kazakhstan, new railroads are being constructed, and existing ones are being reconstructed, alongside the modernization of infrastructure. One of the strategic goals is the expansion of the network for high-speed and very high-speed train services. Organizing such services within the railway network of the Republic of Kazakhstan is closely related to ensuring the required level of reliability of rolling stock and railway tracks, which significantly impacts the safety of train operations [3].

Analysis of scientific and technical sources shows that considerable attention is being paid to improving the reliability of locomotives, however, many studies focus on failures of power plants and electrical systems, while problems related to wear, fatigue and destruction of load-bearing structural elements have not been studied deeply enough [4-8]. Modern works consider individual cases of failures of frames, beams, and connecting nodes, but there is no systematic approach to classifying failures and quantifying them during operation.

The purpose of this article is to analyze the classification of failures of load-bearing parts of locomotives, identify patterns of their occurrence, and develop methodological approaches to predicting the resources and reliability of these elements.

The scientific novelty of the work lies in the systematization of known types of failures of bearing parts, taking into account operating conditions, as well as in the application of a comprehensive reliability forecasting method, including statistical data processing, computational models, and elements of technical diagnostics. The results obtained can be used to optimize maintenance regulations, improve design solutions, and enhance the overall reliability of locomotive rolling stock.

2. Materials and Methods

The probability of fulfilling this condition is characterized by the shaded area in the Figure 1. If, following Gilodo, et al. [9] we assume that the distributions $f(\sigma)$ and $f(\sigma_R)$ can be described by a normal distribution, then the probability of failure-free operation can be calculated using the formula [2, 3].

$$P_B = 0.5 + \Phi\left(\frac{\mu - 1}{\sqrt{v_R^2 \mu^2 + v_o^2}}\right) \quad (1)$$

Here, $\Phi(x)$ is the Laplace function: $\Phi(x) = \int_{-\infty}^x \exp(-0.5 u^2) du$; $\mu = \overline{\sigma_R} / \overline{\sigma}$;

$v_o = S_o / \overline{\sigma}$; $v_R = S_R / \overline{\sigma_R}$; where $\overline{\sigma_R}$, $\overline{\sigma}$, S_o , S_R - the means and root mean square deviations of the operating stresses and strength characteristics.

This method did not gain widespread use because it does not take the time factor into account; it assumes that σ_R and σ are random variables, whereas for the components of the mechanical part of locomotives, the stresses $\sigma(t)$ are random processes [3, 4].

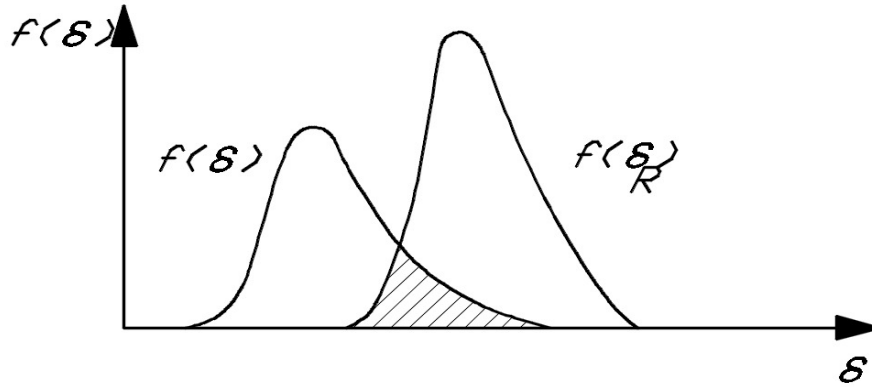


Figure 1.
To the definition of the probability of sudden failure.

The probability of failure-free operation of the load-bearing components subjected to random dynamic stresses, as proposed by Baranovskyi et al. [1], can be estimated by the average number of positive crossings of the random process $\sigma(t)$ through the level σ_R per unit of time. Given that the level σ_R is random and follows the distribution law $f(\sigma_R)$, the probability of failure-free operation should be considered as conditional [4].

$$P_B(t/\sigma_R) = 1 - t f_e \exp[-(\sigma_R - \sigma)^2 / (2S\sigma^2)] \quad (2)$$

To transition from conditional probability to total probability, we use the well-known formula [5]:

$$P_B(t) = \int_{\sigma_{RM}}^{\infty} P_B(t/\sigma_R) f(\sigma_R) d\sigma_R \quad (3)$$

Substituting the expression for the conditional probability here and assuming that the distribution law for $f(\sigma_R)$ follows the Weibull distribution, we get:

$$P_B(t) = 1 - t f_e \frac{\alpha}{q} \int_{\sigma_{RM}}^{\infty} \left(\frac{\sigma_R - \sigma_{RM}}{q} \right)^{\alpha-1} \exp \left\{ -\frac{(\sigma_R - \sigma)^2}{2S\sigma^2} - \left(\frac{\sigma_R - \sigma_{RM}}{q} \right)^\alpha \right\} d\sigma_R \quad (4)$$

Thus, the probability of sudden failures is determined by the random nature of the operating stresses and the strength properties of the components. Similarly, the probability of gradual failures is determined. It is proposed in [9] to calculate this probability based on the expression (3) for the operating time t of a component subjected to a stationary random process $\sigma(t)$, as a function of a single random variable the endurance limit σ_{-1k} .

$$f(t) = f[\sigma_{-1k} = \varphi(t)] \frac{d\varphi(t)}{dt} \quad (5)$$

where $\sigma_{-1k} = \varphi(t)$ — the function inverse to the dependence $t = \psi(\sigma_{-1k})$, according to expression (3);
 $f(\sigma_{-1k})$ — the probability density defined by the expression (3).

Let's rewrite the function $\sigma_{-1k} = \varphi(t)$ based on expression (3) as: $\sigma_{-1k} = \varphi(t) = \sqrt[m]{ct}$ where $c = f_e j_1 (a N_0 \varphi_0^m)^{-1}$

In this case,

$$\frac{d\varphi}{dt} = \frac{\frac{m}{\sqrt[m]{c}}}{m \sqrt[m]{t^{m-1}}} = \frac{m}{m} t^{(1-m)m} \quad (6)$$

Then,

$$f(t) = \frac{\alpha \sqrt[m]{c}}{mq} t^{(1-m)m} \left(\frac{\sqrt[m]{t} - t_M}{q_t} \right)^{\alpha-1} \exp \left[-\left(\frac{\sqrt[m]{t} - t_M}{q_t} \right)^\alpha \right] \quad (7)$$

The probability of failure-free operation will be determined by the expression:

$$P(t) \int_t^{\infty} f(t) dt = \exp \left[-\left(\frac{\sqrt[m]{t} - t_M}{q_t} \right)^\alpha \right] \quad (8)$$

where $t_m = \sigma_{-1k} / \sqrt[m]{c}$; $q_t = q / \sqrt[m]{c}$

However, as is well known, the random processes of loading the load-bearing components of locomotives are not stationary, not only due to the dependence of the mean square deviations, effective frequency, and wideband coefficient on the speed of movement, but also due to the influence of changes in track curvature and slope, and most importantly, changes in track characteristics determined by its design and technical condition. The dashed lines in Figure 1 represent 99.7% of the range of variation of the dependencies. S_o , $f_e(v)$, and $\vartheta(v)$, which follow a normal distribution law. This feature leads to the need for developing specific methods for predicting the reliability of railway rolling stock components [6].

2.1. Prediction of the Reliability of Locomotive Mechanical Parts in the Case of Sudden Failures

In the assessment of the long-term static and impact strength of mechanical components, the reserve factor is commonly used. We will assume that a sudden failure of these components corresponds to a reserve factor n_{ct} or n_{yct} that is smaller than the allowable value $[n_{ct}]$ or n_{ct} . The reserve factor n_{ct} will be considered as the ratio of two random variables [7].

$$n_{ct}(L) = \sigma_R / \sigma_{\text{act}}(L) \geq [n_{ct}]. \quad (9)$$

where σ_R is defined by the expression (3);

σ_{act} is the probability density function of the random variable.

The probability density function of the random variable σ_{act} is defined by the distribution law of absolute maxima, taking into account the variability of values. S_o , f_e , σ_m caused by the non-stationary nature of the applied stresses [10].

Thus, the reserve factor n_{ct} can be considered as a deterministic function of two random variables: σ_R and σ_{act} . The function and probability density of n_{ct} can be found based on the general formula. If y is a function of independent random variables z_i , then

$$F(y) = \int_{\Omega} \dots \int f(z_1)f(z_2) \dots f(z_n) dz_1 dz_2 \dots dz_n \quad (10)$$

where $f(z_i)$ — is the probability density function of the random variables Z_i ; Ω — is the domain that defines the correspondence between the possible values of Y and Z_1, Z_2, \dots, Z_n

In the considered case, for the function of two random variables

$$F(n_{ct}; L) = \int_{\Omega} \int f(\sigma_R)f(\sigma_{\text{act}}; L) d\sigma_R d\sigma_{\text{act}} \quad (11)$$

The integration domain Ω is determined based on the following considerations. Suppose that the equivalent operating stress can vary from 0 to ∞ . Then, according to (4) σ_R can vary from 0 to $n_{ct}\sigma_{\text{act}}$ and the double integral in Equation 5 can be replaced by a repeated one [11]:

$$F(n_{ct}; L) = \int_0^{\infty} f(\sigma_{\text{act}}; L) \int_0^{n_{ct}\sigma_{\text{act}}} f(\sigma_R) d\sigma_R d\sigma_{\text{act}} \quad (12)$$

The inner integral in this expression represents the value of the distribution function of the strength characteristic at $\sigma_R = n_{ct}\sigma_{\text{act}}$, i.e.

$$\int_0^{n_{ct}\sigma_{\text{act}}} f(\sigma_R) d\sigma_R = F(\sigma_R = n_{ct}\sigma_{\text{act}}) \quad (13)$$

Taking this into account, expression (13) can be rewritten as:

$$F(n_{ct}; L) = \int_0^{\infty} f(\sigma_{\text{act}}; L) F(\sigma_R = n_{ct}\sigma_{\text{act}}) d\sigma_{\text{act}} \quad (14)$$

Since failure is defined as a decrease in the strength reserve factor below the allowable value (4), the probability of failure occurrence is [10]:

$$F(L) = F(n_{ct} \leq [n_{ct}]; L) = \int_0^{\infty} f(\sigma_{\text{act}}; L) F(\sigma_R = [n_{ct}]\sigma_{\text{act}}) d\sigma_{\text{act}} \quad (15)$$

The probability of failure-free operation, as the probability of the opposite event, is determined by the expression [12]:

$$P(L) = 1 - F(L) = 1 - \int_0^{\infty} f(\sigma_{\text{act}}; L) F(\sigma_R = [n_{ct}]\sigma_{\text{act}}) d\sigma_{\text{act}} \quad (16)$$

Considering that $F(\sigma_R = [n_{ct}]\sigma_{\text{act}})$, According to expression (16), it can be described by the Weibull distribution law

$$F(\sigma_R) = [n_{ct}] \sigma_{3ct} = 1 - \exp \left\{ - \left(\frac{[n_{ct}] \sigma_{3ct} - \sigma_{RM}}{q} \right)^a \right\} \quad (17)$$

Finally, we obtain

$$P(L) = \int_0^\infty \exp \left\{ - \left(\frac{[n_{ct}] \sigma_{3ct} - \sigma_{RM}}{q} \right)^a \right\} f(\sigma_{3ct}; L) d\sigma_{3ct} \quad (18)$$

Similarly, the probability of failure-free operation in the case of a sudden failure associated with the violation of the impact strength condition can be determined as [13].

$$n_y = \sigma_t / \sigma_{3y} \geq [n_{yA}] \quad (19)$$

It should be noted that the distribution law of the quantity σ_{3y} is determined by the formula

$$f(\sigma_{3y}) = \int_{\sigma_{CTM}}^{\sigma_{CT6}} f(\sigma_{CT}) \int_{\sigma_{YM}}^{\sigma_{Y6}} f(\sigma_y) d\sigma_{CT} d\sigma_y \quad (20)$$

where $f(\sigma_y)$ is the probability density function of the impact stresses, which, in the first approximation, can be assumed to be normal; the indices "b" and "m" represent the maximum and minimum values of the corresponding random variables [13]. The values of the distribution moment indicators are shown in Table 1.

Table 1.
Values of indicators of distribution moments.

Material	Moments of the distribution		
	$S(z_i)$	$\mu_3(z_i)$	$\mu_4(z_i)$
Rolling	$0.07 \bar{z}_i$	$0.395 S^3(z_i)$	$3 S^4(z_i)$
Casting	$0.043 \bar{z}_i$	$0.248 S^3(z_i)$	$3 S^4(z_i)$

Reliability prediction in the case of sudden failures can also be performed using the sensitivity theory method [14]. In this case, the moments of the distribution $f(\sigma_{3ct})$ can be determined through calculations using expressions (4) and (9), while the moments of the distributions σ_τ and σ_B can be determined from experimental data or according to Table 1.

The sensitivity functions L to the variation of the random variables can be determined from the formulas (4) and (9):

$$\frac{\partial n(\overline{\sigma_R}, \overline{\sigma_3})}{\partial \sigma_R} = \frac{1}{\sigma_3}; \quad \frac{\partial^2 n(\overline{\sigma_R}, \overline{\sigma_3})}{\partial \sigma_R^2} = 0 \quad (21)$$

$$\frac{\partial n(\overline{\sigma_R}, \overline{\sigma_3})}{\partial \sigma_3} = -\frac{1}{\sigma_3^2}; \quad \frac{\partial^2 n(\overline{\sigma_R}, \overline{\sigma_3})}{\partial \sigma_3^2} = \frac{2\overline{\sigma_R}}{\sigma_3^3} \quad (22)$$

2.2. As An Example, Let's Consider the Results of Reliability Prediction for The Dynamic Models of the Spring Suspension Components

During the manufacturing and operation of locomotives, due to the variation in the characteristics of the materials used for the mechanical parts and deviations in the manufacturing technology of these components, actual values of quality indicators deviate from their calculated and even standard values. For example, the spring stiffness of the suspension system can differ by 30% within the manufacturing tolerances and material properties [13, 14]. Measurements of the stiffness of the spring sets in the suspension systems of electric locomotives showed that the average values $\bar{\kappa}_{1+2}$ are close to the calculated values, while the variation coefficient $v = 5(\text{ж})/\bar{\kappa}$ are approximately 0.047 for the axle suspension and 0.035 for the body suspension. There is also significant variation in the characteristics of hydraulic and frictional vibration dampers. This leads to the fact that the permissible dynamic load for different locomotives of the same type will be different, and even a newly manufactured locomotive may not meet the requirements and allowable values of the PDK. Additionally, changes in the parameters of the spring suspension can occur during operation due to wear of the friction pairs in the frictional vibration dampers, as well as in other mechanical components, such as fluid leakage in hydraulic dampers, aging of rubber elements, etc. During operation, the characteristics of the track also change. Experiments conducted on operating electric locomotives showed that after 7,500 km of travel, the average damping coefficient β decreased by a factor of 1.2, and its standard deviation increased by a factor of 2. Similar changes were found for the frictional force in the vibration dampers. Specifically, for the dampers in electric locomotives, it can be approximated that the average value of the frictional force, in kN, decreases as a function of the distance traveled L in km:

$$\bar{F}_{Tp}(L) = 5.4 - 2.04 * 10^{-5} L \quad (23)$$

All of these factors combined lead to the deterioration of dynamic characteristics during operation. To select the parameters of the spring suspension system that ensure the required quality level over a certain service life or between repairs (operating time), taking into account the aforementioned causes, reliability theory methods are applied. We will limit our

consideration to evaluating one of the main reliability properties, failure-free operation. We will assume that any exceeding of the regulatory value U_i by any of the dynamic quality indicators $[U_i]$ during operation can be regarded as a malfunction of the spring suspension, i.e., as a failure (violation of the vibration protection function).

Statistical characteristics of the permissible dynamic load as functions of random variables, i.e., the parameters κ_k, β_k and F_{TPK} , can be obtained by finding the probability density function of the random variables, or using simplified methods. Among these, the most widely used is the sensitivity theory method, according to which the nonlinear dependence $U_l = U_l(\kappa_k, \beta_k, F_{\text{TPK}}) = U_l(\xi)$ for $l = 1, 2, \dots, n_l; k = 1, 2, \dots, n_k; j = 1, 2, \dots, n_j$; can be expanded in a Taylor series around the mean values of the parameters $\bar{\kappa}_k, \bar{\beta}_k$ and \bar{F}_{TPK} . This allows a relatively simple determination of the moments of the distributions of any order for the function U_l . Here, the following notation is used:

- n_j — the number of determined permissible dynamic loads;
- n_k — the number of corresponding parameters;
- n_j — the total number of random parameters.

Dynamic models of spring suspension components. When analyzing the vibration protection properties of rolling stock in the frequency domain, the so-called dynamic stiffness of the spring suspension is used, which allows for a relatively simple description of the oscillatory processes of the system under investigation.

The generalized dynamic model of the elastic-dissipative element of the spring suspension is shown in Figure 3. It accounts for the possibility of using springs with hydraulic and pneumatic vibration dampers, as well as pneumatic springs. By setting certain parameters $\kappa_{0i}, \beta_{0i}, \kappa_{i0}, \beta_{i0}, \kappa_{i0}$ and β_{i1} (where i is the index for the spring suspension) equal to zero, one can obtain a suspension scheme with a spring and hydraulic vibration damper connected in parallel (Figure 3a), or a scheme consisting of a spring and a parallel-connected elastically isolated hydraulic damper (Figure 3b). Figures 3c and 3d show suspension schemes using pneumatic elements, obtained in the same way from the original scheme in Figure 3. In this case, the scheme in Figure 3c corresponds to the use of a pneumatic damper with a metal housing in the spring suspension, while Figure 3d represents a pneumatic spring without accounting for the stiffness of the rubber-cord shell. When κ_{i0} and β_{0i} are zero, we obtain a suspension scheme. It should be noted that the parameters of the schemes shown in Figure 3 are uniquely determined by the design data of the pneumatic elements. In the general case, the dynamic stiffness of the i -th stage of the spring suspension shown in Figure 4 is determined by the following expression:

$$\kappa_i(j\omega) = \frac{\kappa_{0i}(j\omega)\kappa_{i0}(j\omega)}{\kappa_{0i}(j\omega) + \kappa_{i0}(j\omega)} + \kappa_{i1}(j\omega) \quad (24)$$

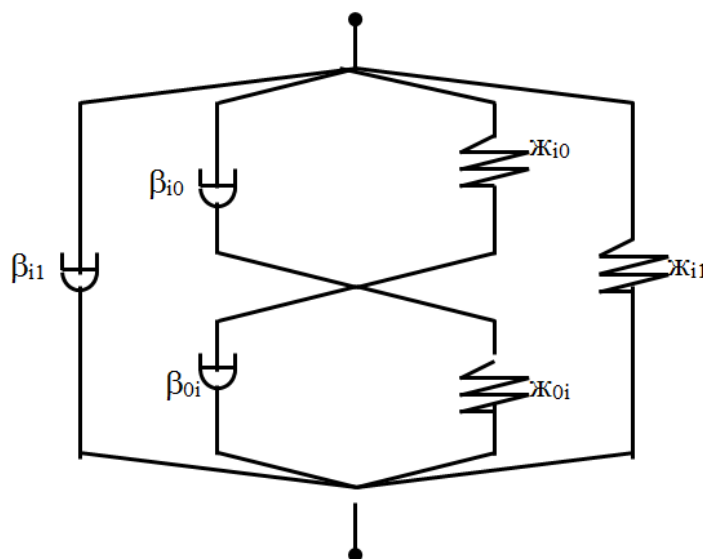
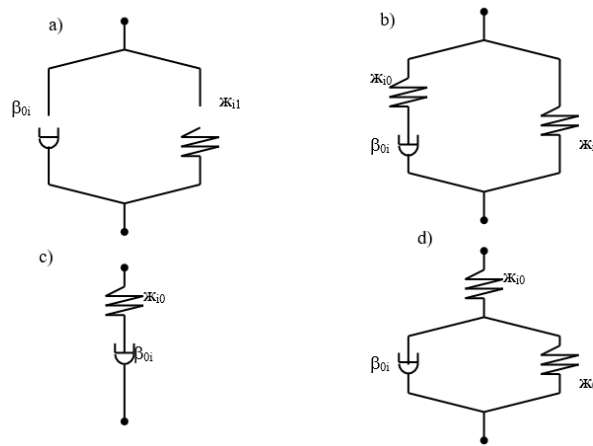


Figure 2.

The scheme of the generalized dynamic stiffness $\kappa_i(j\omega)$.



$$\mathcal{K}_{i1}(j\omega) = \mathcal{K}_{i1} + j\omega\beta_{i1}$$

$$\mathcal{K}_{0i}(j\omega) = \mathcal{K}_{0i} + j\omega\beta_{0i}$$

$$\mathcal{K}_{i0}(j\omega) = \mathcal{K}_{i0} + j\omega\beta_{i0}$$

Figure 3.

Diagram of the spring suspension using springs and a hydraulic damper (a), springs and an elastically isolated hydraulic damper (b), a pneumatic damper with a metal housing (c), and a pneumatic spring (d).

The index "zero" defines the position of the corresponding flexible and damping element in the dynamic model of the spring suspension, while the index "i" denotes the stage number of the suspension. Thus, $i=1$ corresponds to the primary (axle) suspension, and $i=2$ corresponds to the secondary (body) suspension. Since some types of rolling stock have frictional vibration dampers or leaf springs in the axle stage of the spring suspension, it is necessary to introduce linearized values of the damping coefficients of the corresponding nonlinear elements into the calculation scheme (Figure 3a) for the dynamic stiffness of the axle suspension. Based on the method of statistical linearization, the linearized values of the damping coefficients $\beta_{\gamma j}$ can be determined from the condition of equal variances at the output of the nonlinear element before and after the equivalent linear transformation using the following formulas: for the frictional vibration damper.

$$\beta_{\gamma j} = \frac{2F_{TP}}{\sqrt{2\pi S\Delta j}} \quad (25)$$

For the leaf spring

$$\beta_{\gamma j} = \frac{2f_{cm}\mathcal{K}\varphi}{\sqrt{2\pi S\Delta j}} \quad (26)$$

where F_{mp} - the magnitude of the dry friction force of the frictional vibration damper;

$S\Delta j$ - standard deformation rate of the nonlinear element;

f_{cm} - static deflection of the leaf spring;

\mathcal{K} - stiffness of the leaf spring;

φ - friction coefficient of the leaf spring;

j - the number of the nonlinear element corresponding to the wheel or wheelset number of the investigated rolling stock.

Expressions (3) and (4) are given for the centered process Δj . Since $S\Delta j$ is unknown and can only be determined after solving the problem, the method of successive approximations must be applied to determine $\beta_{\gamma j}$. This method is implemented as follows: In the model of the investigated system (rolling stock-track), an arbitrary value $\beta_{\gamma j}(K)$ is chosen, for which the standard deviation $S\Delta j$ is calculated. For the obtained value of $S\Delta j$, the value $\beta_{\gamma j}(K+1)$ is determined using formulas (3) or (4), depending on the type of vibration damper. The iterative process ends $\left| 100(\beta_{\gamma j}(K+1) - \beta_{\gamma j}(K)) / \beta_{\gamma j}(K) \right| \leq \varepsilon$ when the inequality is satisfied, where $\varepsilon=3\%$.

3. Results of the Dynamic Model of the Pneumatic Vibration Damper

The conducted studies showed that the linearized values of the damping coefficients of the axle suspension $\beta_{\gamma j}$ differ from each other by no more than 5-6%. This fact allows linearization of systems based on a single nonlinear element, leading to significant savings in machine time. Thus, the model of the generalized dynamic stiffness of the spring suspension allows a relatively simple way to account for the possibility of applying, in the spring suspension of the investigated dynamic systems, almost all major types of existing linear or linearized elastic and dissipative connections. The pneumatic vibration

damper has characteristics more favorable for damping oscillations of the rolling stock than the hydraulic damper, which has been widely used for this purpose. This is because the damping ability of the pneumatic damper increases much more slowly with frequency compared to the hydraulic damper, and then, after reaching a maximum, it decreases. In addition, the pneumatic vibration damper has a simpler design and greater stability of characteristics than the hydraulic one. The paper provides relationships that allow the selection of parameters for the pneumatic vibration damper depending on its damping ability; however, the mathematical model of the damper was not considered. Therefore, in this work, the author made an attempt to identify the structure and parameters of the dynamic model of the pneumatic damper, i.e., to obtain a mathematical model that would allow the study of the oscillations of the rolling stock. The solution to this problem was based on the results of a field experiment obtained during tests of the pneumatic damper at an experimental site in a depot. The schematic of the damper setup used in these tests is shown in Figure 3. The disturbance during these tests was sinusoidal displacement of the upper part of the damper, $z(t) = z_0 \sin 2\pi ft$ and the output coordinate was taken as the force $Q_3(t)$ in the piston rod of the damper, measured by wire strain gauges 1 and 2. The damper tests were conducted at four different values of disturbance amplitude $z_0=5, 10, 15, 20$ mm. The force in the piston rod was also found to be very close to sinusoidal, indicating the possibility of describing the system with a linear model. As a result of the experiment, the dependencies of the dynamic force $Q_3(f)$ on the disturbance frequency and the phase frequency characteristic (PFC) $\varphi_3(f)$ of the damper, which defines the phase lag of the force $Q_3(t)$ relative to the disturbing influence $z(t)$, were determined.

For the identification of the structure of the model of the pneumatic damper, the dependency $Q_3(f)$ was recalculated into the amplitude-frequency characteristic (AFC) of the damper from displacement to force:

$$A_3(f) = \frac{Q_3(f)}{Z_0} \quad (27)$$

where Z_0 - amplitude of the input disturbance $Z(t)$;

f - frequency of the input disturbance, Hz.

Figures 4–6 show the graphs of the AFC and PFC for different values of the throttle hole diameter d , charging air pressure P_0 , and the amplitude of the input disturbance. It can be assumed that the graphs of $A_3(f)$ and $\varphi_3(f)$, obtained at different values of Z_0 , practically coincide, and the discrepancies between them can probably be explained by a slight dependence of these characteristics on Z_0 . The practical coincidence of the graphs of $A_3(f)$ and $\varphi_3(f)$ at different values of Z_0 indicates that the damper model is close to linear [15].

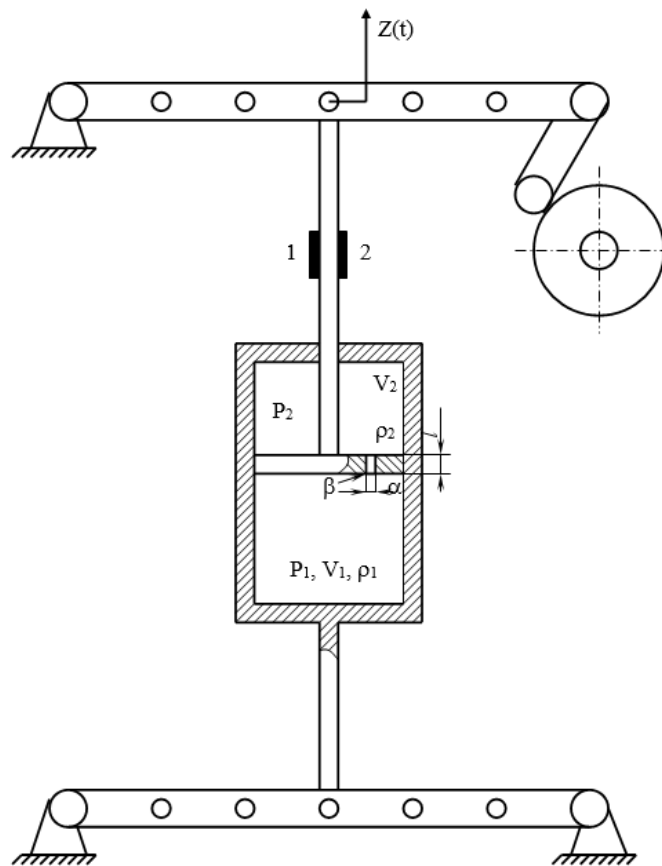


Figure 4.
Schematic diagram of the pneumatic vibration damper setup on the vibration stand.

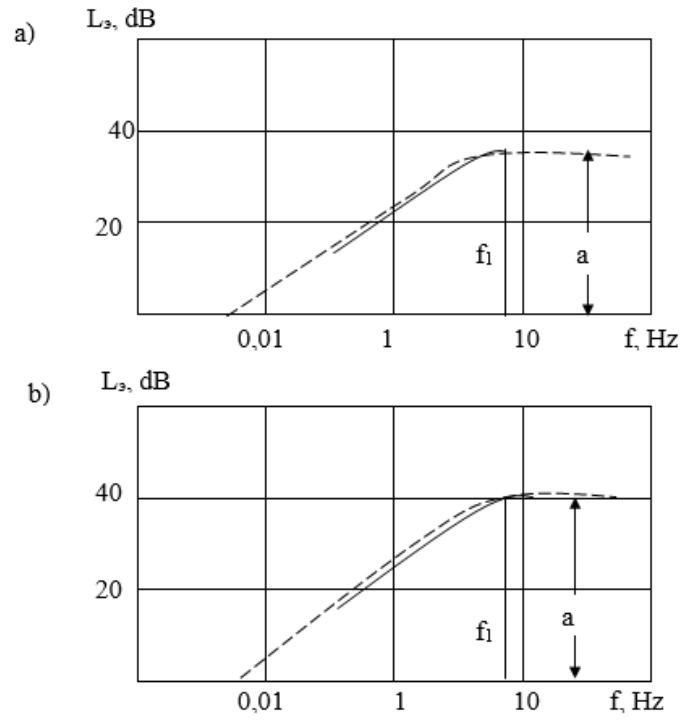


Figure 5. Logarithmic amplitude frequency characteristics at $P_0=0.6$ MPa (a), $P_0=0.8$ MPa (b) and $d=5$ mm.

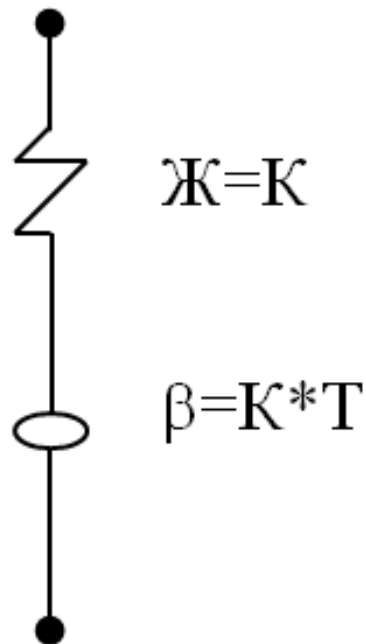


Figure 6. The scheme of replacing the pneumatic damper with a mechanical analog.

To choose the structure of the damper model, based on the averaged dependence of $A_3(f)$, $L_3(f)$, the logarithmic amplitude frequency characteristics (LAFCH), widely used in automatic control theory, were constructed:

$$L_3(f) = 20 \lg A_3(f) \quad (28)$$

For example, in Figure 6, the graphs of $L\vartheta(f)$ are shown, constructed for $P_0=0.6$ MPa and $P_0=0.8$ MPa, and $d=5$ mm. The asymptotic characteristics are shown by a dashed line, with the left branch having a slope of +20 dB/decade (1 decade corresponds to a tenfold change in frequency). This type of logarithmic amplitude-phase frequency response closely corresponds to a dynamic link with a frequency response [14]:

$$W(j2\pi f) = \frac{jK2\pi fT}{1 + j2\pi fT} \quad (29)$$

for which the frequency characteristic is:

$$\begin{aligned} A(2\pi f) &= \frac{K2\pi fT}{\sqrt{1 + (2\pi f)^2 T^2}} \\ \varphi(2\pi f) &= 90^\circ - \arctg(2\pi fT) \end{aligned} \quad (30)$$

Where:

$$T = \frac{1}{2\pi f_1}, \quad K = A \lg \frac{a}{20}$$

($A \lg(\bullet)$ represents the antilogarithm of the corresponding number).

The electrical analog of such a link, and the mechanical analog is the series connection of springs with stiffness K and a hydraulic damper with a damping coefficient $\beta=KT$. The dynamic stiffness of this replacement scheme will be as follows [15]:

$$\kappa(j\omega) = \frac{K}{1 + \frac{K}{j\omega\beta}} \quad (31)$$

In the numerator of the fractional values presented in Table 2, the values obtained through the identification of the pneumatic damper parameters are indicated, while in the denominator, the values obtained using the methodology are given.

Table 2.

The values of the pneumatic damper parameters.

The value of the charging pressure and the diameter of the throttle hole		The values of the parameters			
P_0 , MPa	d , m	K , kN/m	T , s	β , kN·s/m	f_1 , Hz
0.6	0.004	689/734	0.0690/0.0594	47.5/43.6	2.30/2.68
	0.005	785/734	0.0339/0.0286	26.6/21.0	4.69/5.56
0.8	0.004	981/943	0.0503/0.0462	49.3/43.6	3.16/3.44
	0.005	1050/943	0.0234/0.0223	24.6/21.0	6.80/7.14

4. Discussion

The performed analysis shows that the main types of failures of the bearing parts of locomotives are fatigue failures, corrosion wear, mechanical deformations, and failure of welded joints. Failures are most often recorded in the elements of the trolley frame, side beams, and suspension elements due to both high cyclic loads and the influence of aggressive external factors.

The results of processing the operational data confirmed that fatigue cracks form mainly in places of stress concentration in areas of welds, holes, and cross-section junctions. Corrosion damage is more often observed during prolonged operation in conditions of high humidity and poor sealing of components. This confirms the need for regular monitoring and timely maintenance of the load-bearing elements.

The use of forecasting methods based on operating time to failure has made it possible to predict the probability of failure of individual components with maximum accuracy. Models that take into account a range of factors, such as load, locomotive mileage, climatic conditions, and scheduled repairs, are particularly effective. This approach enables a transition to predictive maintenance, which can significantly improve the overall reliability of locomotives and reduce unplanned downtime.

The results obtained indicate the need to optimize the locomotive maintenance system. In particular, it is proposed to introduce regular non-destructive testing in critical areas of structures, the use of materials with increased fatigue strength and corrosion resistance, as well as the development of digital health monitoring systems.

The identified failure rates and the successful testing of predictive models create the prerequisites for improving the efficiency of locomotive operation, increasing repair intervals, and reducing operating costs.

5. Conclusions

The obtained results were used in the analysis of the experimental study of the pneumatic shock absorber's performance in a dynamic system with one degree of freedom. These results, in the form of an experimental amplitude-frequency characteristic $A_\vartheta(f) = \varphi_{02}/\varphi_{01}$, where φ_{01} and φ_{02} are the amplitudes of the disturbance and angular oscillations of the balance with the attached mass m , respectively, were compared to the theoretical $A_T(f)$ graph. The dependence $A_T(f)$ was obtained from the balancing equation of a spring with stiffness $\kappa=800$ kN/m and a pneumatic shock absorber with parameters $K=785$ kN/m and $T=0.0339$ s, which corresponds to $P_0=0.6$ MPa and $d=5$ mm. The proposed methodology for determining the dynamic stiffness of the pneumatic shock absorber based on the identification of the structure and parameters of the

dynamic model from experimental frequency characteristics allowed the development of a substitute scheme for the pneumatic shock absorber. The verification of the dynamic stiffness properties of the pneumatic shock absorber based on experimental data showed both qualitative and quantitative agreement with the theoretical calculations.

The task of selecting optimal parameters for the suspension system of electric locomotives is advisable to solve using single-criterion optimization methods with sliding tolerance, utilizing the average number of positive deviations per unit of time within the four-dimensional region of allowable states as the objective function. If global optimization is required, a multi-criteria optimization algorithm should be applied, using the LP τ -sequence points for subsequent Pareto solution ranking based on total allowable losses.

By adjusting the parameters of pneumatic shock absorbers in the central and box suspensions within constructively permissible limits, an optimal system can be created with dynamic quality indicators similar to those found in systems with hydraulic shock absorbers.

References

- [1] D. Baranovskyi, M. Bulakh, A. Michajłyszyn, S. Myamlin, and L. Muradian, "Determination of the risk of failures of locomotive diesel engines in maintenance," *Energies*, vol. 16, no. 13, p. 4995, 2023. <https://doi.org/10.3390/en16134995>
- [2] S. Abdullayev, G. Bakyt, A. Kamzina, K. Sarsanbekov, and A. Abdullayeva, "Interaction of the TE33a diesel locomotive and the railway track on curved section with radius 290 m," *Communications-Scientific Letters of the University of Zilina*, vol. 25, no. 4, pp. B315-B326, 2023. <https://doi.org/10.26552/com.C.2023.069>
- [3] A. Bekisz, M. Kowacka, M. Kruszyński, D. Dudziak-Gajowiak, and G. Debita, "Risk management using network thinking methodology on the example of rail transport," *Energies*, vol. 15, no. 14, p. 5100, 2022. <https://doi.org/10.3390/en15145100>
- [4] M. Sejkorová, I. Hurtová, P. Jilek, M. Novák, and O. Voltr, "Study of the effect of physicochemical degradation and contamination of motor oils on their lubricity," *Coatings*, vol. 11, no. 1, p. 60, 2021. <https://doi.org/10.3390/coatings11010060>
- [5] G. Imasheva, S. Abdullayev, N. Tokmurzina, N. Adilova, and G. Bakyt, "Prospects for the use of gondola cars on bogies of model ZK1 in the organization of heavy freight traffic in the Republic of Kazakhstan," *Mechanics*, vol. 24, no. 1, pp. 32-36, 2018. <https://doi.org/10.5755/j01.mech.24.1.17710>
- [6] M. Leite, M. A. Costa, T. Alves, V. Infante, and A. R. Andrade, "Reliability and availability assessment of railway locomotive bogies under correlated failures," *Engineering Failure Analysis*, vol. 135, p. 106104, 2022. <https://doi.org/10.1016/j.engfailanal.2022.106104>
- [7] S. F. Seyedan Oskouei, M. Abapour, and M. Beiraghi, "Identifying critical components for railways rolling stock reliability: a case study for Iran," *Scientific Reports*, vol. 14, no. 1, p. 12080, 2024. <https://doi.org/10.1038/s41598-024-62841-2>
- [8] M. Mussabekov, G. Bakyt, A. Omirbek, E. Brumerčíková, and B. Buková, "Shunting locomotives fuel and power resources decrease," presented at the MATEC Web of Conferences, 2017, 134, 00041. <https://doi.org/10.1051/mateconf/201713400041>, 2017.
- [9] O. Gilodo, A. Arsirii, and Y. Somina, "Analysis of reticulated dome with universal connector," 2024.
- [10] S. Abdullayev, N. Tokmurzina-Kobernyak, G. Ashirbayev, G. Bakyt, and A. Izbaïrova, "Simulation of spring-friction set of freight car truck, taking into account track profile," *International Journal of Innovative Research and Scientific Studies*, vol. 7, no. 2, pp. 755-763, 2024. <https://doi.org/10.53894/ijirss.v7i2.2883>
- [11] S. Bahrami, M. Rastegar, and P. Dehghanian, "An fbwm-topsis approach to identify critical feeders for reliability centered maintenance in power distribution systems," *IEEE Systems Journal*, vol. 15, no. 3, pp. 3893-3901, 2020.
- [12] E. Gascard and Z. Simeu-Abazi, "Quantitative analysis of dynamic fault trees by means of Monte Carlo simulations: Event-driven simulation approach," *Reliability Engineering & System Safety*, vol. 180, pp. 487-504, 2018. <https://doi.org/10.1016/j.res.2018.07.011>
- [13] O. Golbasi and M. O. Turan, "A discrete-event simulation algorithm for the optimization of multi-scenario maintenance policies," *Computers & Industrial Engineering*, vol. 145, p. 106514, 2020. <https://doi.org/10.1016/j.cie.2020.106514>
- [14] G. Bakyt, Y. Jailaubekov, S. Abdullayev, G. Ashirbayev, and I. Ashirbayeva, "Assessment of carbon dioxide emissions in road transport, using exhaust gas cleaning technology, in the Republic of Kazakhstan," *Vibroengineering Procedia*, vol. 48, pp. 87-92, 2023. <https://doi.org/10.21595/vp.2023.23163>
- [15] H. Sun *et al.*, "Preventive maintenance optimization for key components of subway train bogie with consideration of failure risk," *Engineering Failure Analysis*, vol. 154, p. 107634, 2023. <https://doi.org/10.1016/j.engfailanal.2023.107634>